LA-UR-14-21712
CETUP2013-020

Matter-Neutrino Resonance Above Merging Compact Objects

A. Malkus,[1,*] A. Friedland,[2] and G. C. McLaughlin[1,†]

[1] *Department of Physics, North Carolina State University, Raleigh, NC 27695 USA.*
[2] *Theoretical Division, T-2, MS B285, Los Alamos National Laboratory, PO Box 1663, Los Alamos, New Mexico 87545-0285*[‡]

(Dated: March 25, 2014)

Accretion disks arising from neutron star- neutron star mergers or black hole- neutron star mergers produce large numbers of neutrinos and antineutrinos. In contrast to other astrophysical scenarios, like supernovae, in mergers the antineutrinos outnumber the neutrinos. This antineutrino dominance gives neutrinos from merger disks the opportunity to exhibit new oscillation physics, specifically a matter-neutrino resonance. We explore this resonance, finding that consequences can be a large transition of ν_e to other flavors, while the $\bar{\nu}_e$s return to their initial state. We present numerical calculations of neutrinos from merger disks and compare with a single energy model. We explain both the basic features and the conditions for a transition.

PACS numbers: 14.60.Pq1,97.60.Jd,3.15.+g
Keywords: neutrino mixing, neutrinos-neutrino interaction, accretion disk

arXiv:1403.5797v1 [hep-ph] 23 Mar 2014

The merger of two neutron stars or a neutron star and a black hole, forms a black hole accretion disk. These mergers are fascinating for many reasons: as home to large numbers of neutrinos, to dense matter physics [1], jets [2] and gravitational waves [3–5] as well as r-process [6–8] and other types of nucleosynthesis [9–11]. The neutrinos play a significant role in disk dynamics [12], jet production, [13, 14] and wind-type nucleosynthesis [15–17]. Thus the flavor composition of the neutrinos has important consequences, particularly for the outcome of the wind-type nucleosynthesis. Neutrinos, however, can transform away from their flavor composition at emission. We examine the neutrino flavor transformation physics in merger disk neutrinos, and describe a phenomenon which we call a matter-neutrino resonance (MNR) transition.

Neutrino physics has changed dramatically in the past few years. Calculations that take into account the neutrino self-interaction potential in conditions typical of core collapse supernovae have shown that the neutrinos exhibit significant transitions [18–32]. The high density of neutrinos near emission leads to energy synchronized neutrino flavor evolution there [33], Moreover, a remarkable change in flavor occurs further out: As the neutrino self interaction potential drops toward the vacuum scale, $\Delta = \delta m^2/(2E)$, where δm^2 is the mass splitting of the neutrinos and E is their energy [26, 34–36], supernova neutrinos and antineutrinos can oscillate.

Mergers present an oscillation environment not possible in settings studied earlier. Since the material in compact object merger disks begins heavily neutron rich, as it heats it tends to leptonize, i.e. emit more antineutrinos than neutrinos [8, 37, 38]. This has special consequence for the neutrinos because it means that the neutrino self-interaction potential is large and has opposite sign to the matter potential. When the two potentials cancel an MNR transition can occur. A transition at such a resonance point was observed in [39] in the context of disks from stellar collapse. This resonance occurs in both hierarchies, because for these environments, this cancellation point is well above the vacuum scale. In contrast to the supernova neutrino phenomena, neutrinos behave differently than antineutrinos close to the neutrino emission point. Thus a resonance transition can significantly influence wind-type nucleosynthesis above a disk.

In this paper we explain the basic physics of this transition using a single energy model and provide an analytic formula to describe the resulting transition. While the resonance condition is similar to that from stellar collapse disks, the resonance in merger disks causes novel behavior. We present calculations of transformation above merger disks.

Matter-Neutrino Resonance: A single energy model of just a neutrino and an antineutrino is the most straightforward way to explore our resonance. With two flavors and a single energy, the problem can be easily written in the language of the Neutrino Flavor Isospin (NFIS) [40] formalism, named for the neutrino flavor isospin vectors, $\mathbf{s}(\bar{\mathbf{s}})$. These vectors have length 1/2, and the third($\hat{\mathbf{z}}$) components are $s_z = P_{\nu_e} - 1/2 (\bar{s}_z = -P_{\bar{\nu}_e} + 1/2)$, where P_{ν_e} ($P_{\bar{\nu}_e}$) is the survival probability for an electron (anti)neutrino. In NFIS the $\hat{\mathbf{z}}$ component of the potential for the neutrinos is $V_z(t) = 2\mu_\nu (s_z + \alpha \bar{s}_z) + V_e(t) - \Delta \cos 2\theta_V$, where the unoscillated self-interaction potential is $\mu_\nu (1-\alpha) = V_{\nu\nu}$, and the matter potential is $V_e(t)$ (see [32] for the full definitions of these potentials). The unoscillated electron neutrino contribution to the self interaction potential is described by μ_ν and the ratio of the unoscillated antineutrino and neutrino fluxes is α. In

*Electronic address: acmalkus@ncsu.edu
†Electronic address: gcmclaug@ncsu.edu
‡Electronic address: alexfriedland@gmail.com

their entirety, the evolution equations are,

$$\frac{\partial \mathbf{s}}{\partial t} = \mathbf{s} \times [\Delta \mathbf{H}_V + V_e \hat{\mathbf{z}} + 2\mu_\nu(\mathbf{s} + \alpha \bar{\mathbf{s}})] \,, \tag{1}$$

$$\frac{\partial \bar{\mathbf{s}}}{\partial t} = \bar{\mathbf{s}} \times [-\Delta \mathbf{H}_V + V_e \hat{\mathbf{z}} + 2\mu_\nu(\mathbf{s} + \alpha \bar{\mathbf{s}})] \tag{2}$$

where $\mathbf{H}_V = (-\sin 2\theta_V, 0, \cos 2\theta_V)$ depends on the vacuum angle, θ_V. For θ_V we use a value consistent with the recommended value of $\theta_{13} = 0.15$ [41]. The sign of Δ determines the hierarchy. We assume that the neutrinos start in pure flavor states, so $\mathbf{s}$ and $\bar{\mathbf{s}}$ initially point in the $\hat{\mathbf{z}}$ and $-\hat{\mathbf{z}}$ directions. We perform

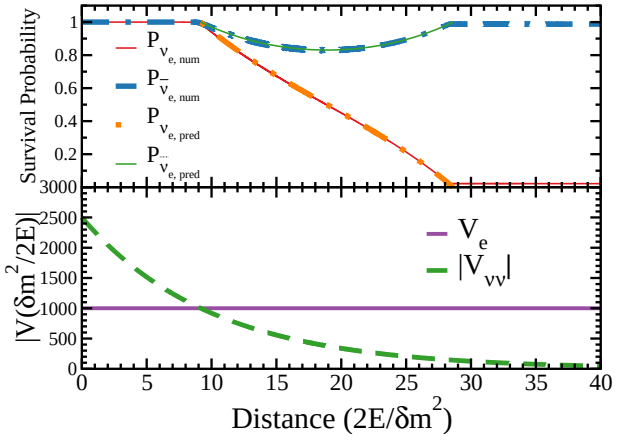

(a)Antineutrinos initially dominate.

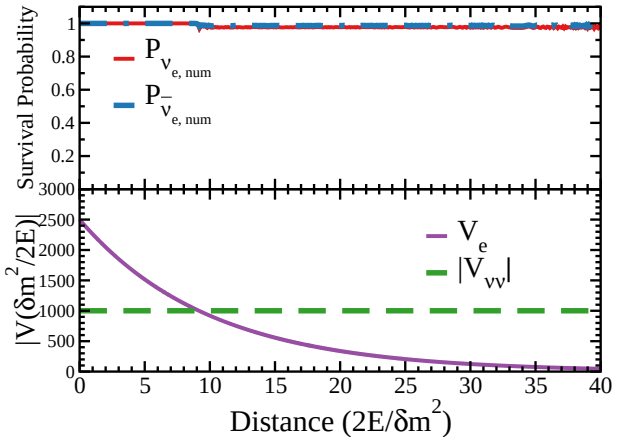

(b)Matter initially dominates.

FIG. 1: *Top panel, both plots*: Survival probabilities P_{ν_e} (solid red line) and $P_{\bar{\nu}_e}$ (dashed blue line). *Bottom panel, both plots*: Potentials in units of Δ. The purple solid line shows the magnitude of the neutrino-electron potential, $V_e(t)$, and the green dashed line shows the unoscillated neutrino-neutrino interaction potential, $|V_{\nu\nu}| = \mu(t)(\alpha - 1)$.

two types of calculations with this single energy configuration. In the first type of calculation, we begin with $V_e(t=0) < |\mu_\nu(t=0)\,(1-\alpha)|$ so that the neutrino self-interaction potential is greater than the matter potential. We then allow μ_ν to decline so that we can pass through the region where $V_e(t) = |\mu_\nu(t)\,(1-\alpha)|$. In the second we start with $V_e(t=0) > |\mu_\nu(t=0)\,(1-\alpha)|$ corresponding to the situation where the matter potential is initially greater than the self-interaction potential. We then allow $V_e(t)$ to decline so that at some point it crosses through the region where $V_e(t) = |\mu_\nu(t)\,(1-\alpha)|$. We demonstrate the results of this calculation in Fig. 1 with the specific functional forms $V_e(t) = 1000\Delta$, $\mu_\nu(t)(\alpha-1) = 10000\Delta e^{\left(-\frac{\Delta}{10}t\right)}$ in Fig. 1(a), and $V_e(t) = 10000\Delta e^{\left(-\frac{\Delta}{10}t\right)}$, $\mu_\nu(\alpha-1) = 1000\Delta$, in Fig. 1(b). In both Figs., $\alpha = 4/3$. The top panels of these plots show that the scenario where $\mu_\nu(t)\,(\alpha-1)$ initially dominates over $V_e(t)$ produces a transition, while the reverse scenario does not.

When there is a significant transition, it takes place over an extended period of time. The form of the potentials will determine how long the system takes to go from the beginning, $V_e(t_i) \approx \mu_\nu(t_i)\,(\alpha-1)$ to the end, $V_e(t_f) \approx \mu_\nu(t_f)\,(1+\alpha)$. The time of the transition is $\delta t_1 \sim \tau_{V_e/\mu} \ln((1+\alpha)/(\alpha-1))$, where $\tau_{V_e/\mu}$ is the effective scale height of the ratio of the matter potential to the neutrino potential,, $\tau_{V_e/\mu} = |d\ln(V_e/\mu_\nu)/dt|)^{-1}$. During this time, the system maintains a position approximately on the resonance, i.e. $V_z(t) \approx V_e(t) + \mu_\nu(t)\,(s_z + \alpha \bar{s}_z)$ hovers around zero. The neutrino and antineutrino transform to maintain a cancellation with the matter term. This behavior differs both from standard MSW [42, 43] where the system passes quickly through the place where $V_z(t) = 0$ and also from synchronized oscillation where the neutrinos and antineutrinos are locked.

In order to understand this transition better, we obtain an analytical expression for the transition behavior. Examining the sum of Eqs. (1) and (2) as well as the behavior in Fig. 1(a), we see that precession around the z-axis is nearly absent so that during the transition $s + \alpha\bar{s}$ grows along the z-axis only. By combining $s_x \approx -\alpha \bar{s}_x$, $s_y \approx -\alpha \bar{s}_y$, and $V_z(t) \approx 0$, along with the approximation $\Delta \approx 0$ we find

$$s_z \approx \frac{\left(\alpha^2 - 1\right)\mu_\nu(t)^2 - V_e(t)^2}{4V_e(t)\mu_\nu(t)} \tag{3}$$

$$\bar{s}_z \approx -\frac{\left(\alpha^2 - 1\right)\mu_\nu(t)^2 + V_e(t)^2}{4\alpha V_e(t)\mu_\nu(t)}. \tag{4}$$

Since $P_{\nu_e} = s_z + 1/2$ and $P_{\bar{\nu}_e} = -\bar{s}_z + 1/2$, we now have an analytical prediction which we can test with our numerical single energy calculation.

In Fig. 1(a), starting at the initial resonance point, we plot our analytic estimate of the survival probabilities from Eqs. (3) and (4). If we try the same for Fig. 1(b), we do not find allowed solutions for the survival probability. This lack of solutions is consistent with what the figures show: if the potential begins matter dominated, little transition occurs, whereas if it begins (anti)neutrino

dominated then significant transformation occurs.

We note, however, that an initially (anti)neutrino potential is not in general sufficient to induce a transition. The mixing angle, θ_V also plays a role. From inspection of the sum of Eqs. (1) and (2), we see that the timescale of the transition is $\delta t_2 \approx \alpha/(\Delta \sin 2\theta_V \langle s_y - \alpha \bar{s}_y \rangle)$, where $\langle \cdot \rangle$ is the average value during the transition. For the timescales, δt_1 and δt_2 to be compatible, $\langle s_y - \alpha \bar{s}_y \rangle$ must adjust to θ_V and $\tau_{V_e/\mu}$, but for some conditions the required adjustment would cause it to become unphysical. Therefore, therefore when $\Delta \sin 2\theta_V$ becomes small the transition is not realized. In the example in Fig. 1(a), if the mixing angle becomes an order of magnitude or more smaller, then little transition occurs.

We note that this phenomenon is similar in both hierarchies, as long as the potentials stay well above the vacuum scale. However, the existence of the transition does depend on the asymmetry between neutrinos and antineutrinos. One way in which this manifests is the in situations where a significant ν_μ and/or ν_τ flux exists as well.

Suppression of the matter-neutrino resonance transition from ν_μ and ν_τ: Disks from compact object mergers will not only emit electron neutrinos and antineutrinos, but also ν_μ, ν_τ, $\bar{\nu}_\mu$, and $\bar{\nu}_\tau$. We explore the importance of ν_μ, ν_τ to the matter neutrino resonance transition, by considering four types of neutrinos, ν_e, $\bar{\nu}_e$, ν_μ and $\bar{\nu}_\mu$, all with the same energy. In Fig. 2 we have taken the model used to make Fig. 1(a), and added to it a muon neutrino and antineutrino of the same energy. In Fig. 2, the fluxes of the muon neutrino and antineutrino are equal. The ratio of the muon neutrino flux relative to the electron neutrino flux is β. We see from these figures that a sufficiently large ν_μ flux suppresses the transition. The bottom panels show that when the system exhibits a transition it maintains the resonance $V_z(t) \approx 0$, but when it does not, $V_z(t)$ passes straight through zero.

Net flavor isospin vectors, e.g. $\mu(t) s_z = \mu_e(s_{\nu_e,z} + \beta s_{\nu_\mu,z})$ are helpful in understanding the behavior in Fig. 2. The net vector is reduced as the flux of muon neutrinos increases and eventually switches sign. Since transition depends on the ability of the NFIS vectors to rotate in such a way that $V_z(t) \approx 0$ is maintained and the x and y components cancel, if the net vector is reduced to almost zero, then this becomes impossible. Therefore, a muon neutrino flux comparable to the electron neutrino flux suppresses the transition. Similarly if the muon antineutrino and electron antineutrino fluxes are comparable then the transition is suppressed.

Merger Disk Calculations: Determining how many neutrinos are emitted from a compact object merger disk is clearly a more complex task. The emission produces an energy spectrum for all types neutrinos ν_e, ν_μ, ν_τ, $\bar{\nu}_e$, $\bar{\nu}_\mu$, and $\bar{\nu}_\tau$. While there are many similarities in the predictions for the flux and energy distributions of ν_e and $\bar{\nu}_e$, the number of emitted μ and τ type neutrinos is less certain. Estimates of the flux of these neutrinos range from comparable to the flux of ν_e to a small fraction $\sim 20\%$ to $\sim 30\%$ [37, 38].

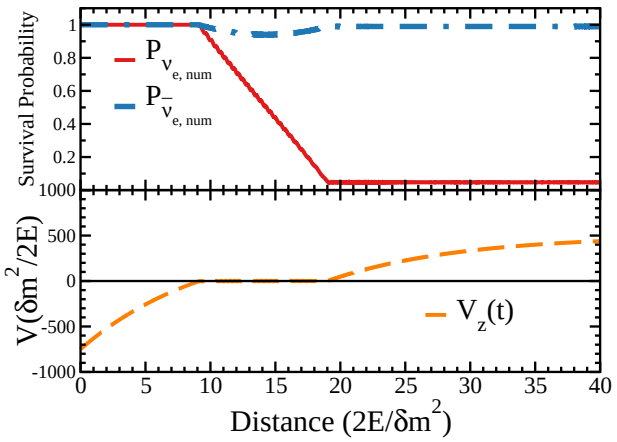

(a)$\beta = 0.7$

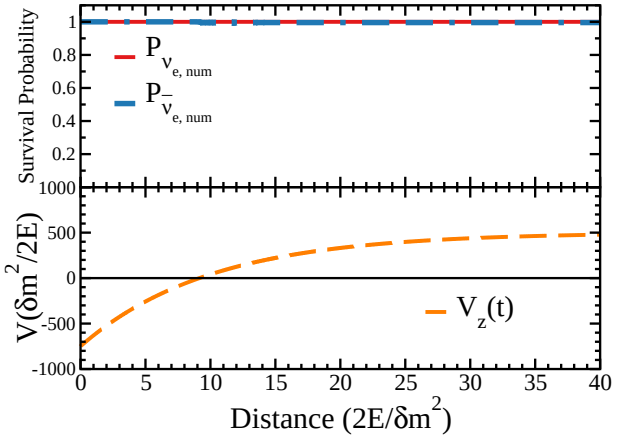

(b)$\beta = 1.3$

FIG. 2: *Top panel, both plots*: Survival probabilities, P_{ν_e} (solid red line) and $P_{\bar{\nu}_e}$ (dashed blue line). *Bottom panel, both plots*: Potentials $V_z(t)$. Fig. 2(a) shows $\beta = 0.7$ and Fig. 2(b) shows $\beta = 1.3$, where β is the ratio of the muon flux to the electron neutrino flux. In both cases the overall potential begins dominated by the neutrino-neutrino interaction term, $V_z(t) < 0$.

Before we perform calculations that address the multi-energy nature of the emitted flux, the complex geometry of the disk, and the emission of all types of neutrinos, we first need to determine representative conditions. Guided by the results of compact object merger neutrino surface calculations, e.g. [44], we construct a disk with the same qualitative features, i.e. the disk emits all types of neutrinos with energy hierarchy, $E_{\nu_e} < E_{\bar{\nu}_e} < E_{\nu_{\mu,\tau}}$ and the number flux of $\bar{\nu}_e$ is largest, followed by ν_e and then $\nu_{\mu,\tau}$. We choose the disk radius to be $R_0 = 4.5 \times 10^6$ cm and temperatures $T_{\nu_e} = 6.4$ MeV, $T_{\bar{\nu}_e} = 7.1$ MeV, and $T_{\bar{\nu}_{\mu,\tau}} = T_{\nu_{\mu,\tau}} = 7.4$ MeV. We assume that neutrinos are not emitted from the last stable orbit, as determined

from a $3M_\odot$ black hole at the center. The disk size is expected to be smaller for the ν_μ and ν_τ than for ν_e. For ease of computation, we use the same disk size for each flavor of neutrino and take account of the smaller ν_μ, $\bar{\nu}_\mu$, ν_τ, $\bar{\nu}_\tau$ fluxes by scaling these fluxes relative to their blackbody values

We generalize the calculation in the previous section to multi-energies and three flavors of neutrinos. We perform a three flavor calculation by numerically solving for the scattering matrices, $S(E,r)$ and $\bar{S}(E,r)$ as described in [45, 46]. We assume that the neutrinos are initially purely in flavor states, use the "single angle" approximation [47], and take the vacuum parameters to be $\delta m^2_{12} = 7.6 \times 10^{-5}\mathrm{eV}^2$, $\delta m^2_{32} = -2.4 \times 10^{-3}\mathrm{eV}^2$, $\theta_{12} = 0.60$, $\theta_{13} = 0.16$ and $\theta_{32} = 0.76$, which are values consistent with the Particle Data Group's favored parameters [48].

We report results in Fig. 3 for a neutrino moving along the same trajectory that might be taken by an outflowing mass element [17], which begins an an initial disk radius of $r_0 = 2.2 \times 10^6$ cm. While the material lifts initially vertically from the disk, it later takes a radial trajectory. Since we are *not* considering a trajectory emitted vertically above the black hole, we *cannot* rely on the disk symmetry to simplify the calculation. Instead, we use the geometric factor that describes the decline of the neutrino fluxes as a function of distance from the disk from [39]. The top panels in Fig. 3(a) and Fig. 3(b) show the energy integrated survival probability. In the bottom panels of each figure, we show the overall relative strengths of each part of the potential, the matter potential $V_e(r)$ and the unoscillated neutrino self interaction potential $|V_{\nu\nu}(r)|$.

The results depicted in Fig. 3(a) confirm that that the MNR transition occurs as predicted. We see that the crossing points A and B produce different behavior. A careful examination of the bottom panel of Fig. 3(a), shows that at crossing point A, the system begins matter dominated, while at crossing point B, it begins neutrino dominated. Consistent with the behavior of the single energy calculation, point A produces no transition, while point B produces a neutrino matter resonance transition. For situations like Fig. 3(a), where the mu/tau contribution is small one can apply the timescale arguments from the single energy model. The asymmetry is $\alpha = 1.37$ and the potential ratio scale height is $\tau_{V_e/\mu} = 5.8 \times 10^6$cm, so the system should exhibit the MNR transition for $\theta \gtrsim 2.3 \times 10^{-2}$, which is safely fulfilled by the measured value of θ_{13} [41]. Again consistent with the single energy calculation, from a comparison of Fig. 3(a), with Fig. 3(b), we see that there is an abrupt change in the transition behavior when the μ and τ type neutrino fluxes become larger than a certain size.

Conclusions In the compact object merger disks, we find that MNR transitions can occur in places where the neutrino self-interaction potential initially dominates the matter potential, but then later the two potentials become comparable. Because of the large measured value

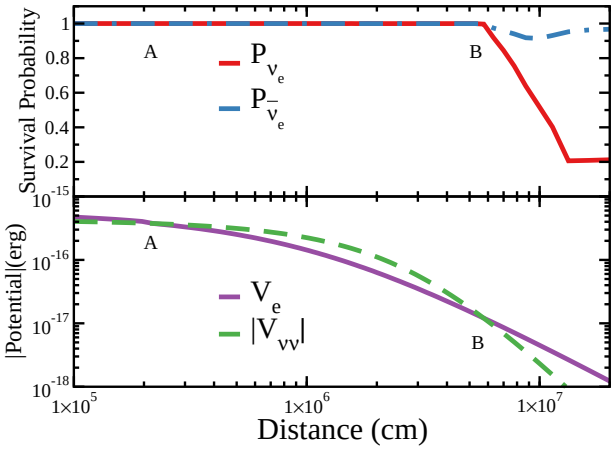

(a)Fluxes of ν_μ, ν_τ, $\bar{\nu}_\mu$, and $\bar{\nu}_\tau$ are scaled so that the emitted number flux is 35% of blackbody.

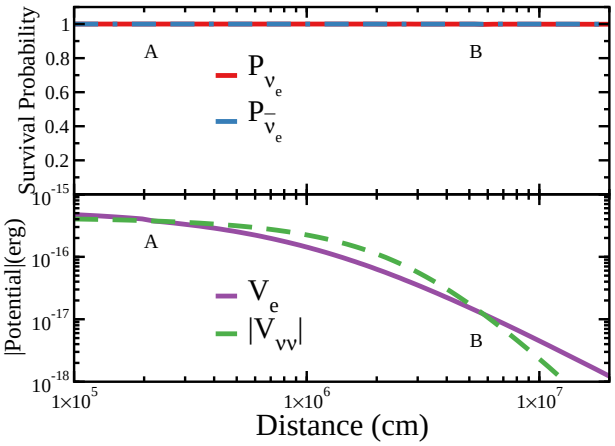

(b)Fluxes of ν_μ, ν_τ, $\bar{\nu}_\mu$, and $\bar{\nu}_\tau$ are scaled so that the emitted number flux is 40% of blackbody.

FIG. 3: *Top panel, both plots*: The solid red (dashed blue) line shows the survival probability for an electron neutrino (antineutrino) as a function of progress along the trajectory. *Bottom panel, both plots*: The solid purple line shows the matter potential, $V_e(r)$ The dashed green line shows the magnitude of the neutrino self interaction potential, $|V_{\nu\nu}|$ in the absence of oscillation. Crossing (resonance) points and are indicated by the letters A and B on the plot.

of θ_{13}, the transition behavior is not finely tuned; it occurs over a wide range of disk radii, densities and neutrino fluxes. The transition can be suppressed by large ν_μ and ν_τ flux, but current calculations predict a relatively small contribution [37, 38].

Since MNR transitions occur relatively close to the surface of the disk, we expect them to influence wind type nucleosynthesis, such as r-process[8] or nickel production [9]. The transition, therefore, could have an observable consequences in the galactic inventory of elements, or in the the electromagnetic signal from mergers, sometimes called a kilonova [49].

Not only must knowledge of the true flux of ν_μ, ν_τ in future models of compact object mergers be gained, but several more outstanding issues in neutrino flavor transformation physics must be resolved in order to fully understand this resonance transition. For example, further study is needed to examine multi-angle, [24, 29–31] and halo effects [50].

We thank J. F. Cherry, Jim Kneller, Rebecca Surman and Cristina Volpe for useful discussion. This work was supported in part by U.S. DOE Grants No. DE-FG02-02ER41216 and de-sc0004786, and in part by the LANL LDRD program. GCM and AF would like to thank CETUP*(Center for Theoretical Underground Physics and Related Areas), for its hospitality and partial support during the 2013 Summer Program.

[1] J. M. Lattimer, Annual Review of Nuclear and Particle Science **62**, 485 (2012),
[2] S. I. Blinnikov, I. D. Novikov, T. V. Perevodchikova, and A. G. Polnarev, Soviet Astronomy Letters **10**, 177 (1984)
[3] G. M. Harry and LIGO Scientific Collaboration, Classical and Quantum Gravity 27, 084006 (2010)
[4] M. D. Duez, Classical and Quantum Gravity **27** 114002 (2010)
[5] T. W. Baumgarte and S. L. Shapiro, Numerical relativity: Solving Einsteins Equations on the Computer (Cambridge University Press, Cambridge, 2010)
[6] J. M. Lattimer, F. Mackie, D. G. Ravenhall, and D. N. Schramm, Astrophys. J. **213** 225 (1977)
[7] S. Rosswog, O. Korobkin, A. Arcones and F. -K. Thielemann, arXiv:1307.2939 [astro-ph.HE].
[8] R. Surman, G. C. McLaughlin, M. Ruffert, H. -T. Janka and W. R. Hix, Astrophys. J. **679**, L117 (2008) [arXiv:0803.1785 [astro-ph]].
[9] R. Surman, O. L. Caballero, G. C. McLaughlin, O. Just and H. -T. Janka, arXiv:1312.1199 [astro-ph.SR].
[10] J. Pruet, R. Surman and G. C. McLaughlin, Astrophys. J. **602**, L101 (2004) [astro-ph/0309673]. [11]
[11] R. Surman, G. C. McLaughlin and N. Sabbatino, Astrophys. J. **743**, 155 (2011) [arXiv:1112.2673 [astro-ph.HE]].
[12] A. MacFadyen and S. E. Woosley, Astrophys. J. **524**, 262 (1999) [astro-ph/9810274].
[13] M. Ruffert and H. T. Janka, Astron. Astrophys. **344**, 573 (1999) [astro-ph/9809280].
[14] R. Oechslin and H. -T. Janka, Mon. Not. Roy. Astron. Soc. **368**, 1489 (2006) [astro-ph/0507099].
[15] R. Surman and G. C. McLaughlin, Astrophys. J. **603**, 611 (2004) [astro-ph/0308004].
[16] R. Surman, G. C. McLaughlin and W. R. Hix, Astrophys. J. **643**, 1057 (2006) [astro-ph/0509365].
[17] R. Surman and G. C. McLaughlin, Astrophys. J. **618**, 397 (2004) [astro-ph/0407206].
[18] A. B. Balantekin and Y. Pehlivan, J. Phys. G **34**, 47 (2007) [astro-ph/0607527].
[19] A. B. Balantekin and H. Yuksel, New J. Phys. **7**, 51 (2005) [astro-ph/0411159].
[20] Y. Pehlivan, A. B. Balantekin, T. Kajino and T. Yoshida, Phys. Rev. D **84**, 065008 (2011) [arXiv:1105.1182 [astro-ph.CO]].
[21] G. G. Raffelt and A. Y. Smirnov, Phys. Rev. D **76**, 081301 (2007) [Erratum-ibid. D **77**, 029903 (2008)] [arXiv:0705.1830 [hep-ph]].
[22] J. Gava and C. Volpe, Phys. Rev. D **78**, 083007 (2008) [arXiv:0807.3418 [astro-ph]].
[23] B. Dasgupta, A. Dighe, G. G. Raffelt and A. Y. Smirnov, Phys. Rev. Lett. **103**, 051105 (2009) [arXiv:0904.3542 [hep-ph]].
[24] H. Duan and A. Friedland, Phys. Rev. Lett. **106**, 091101 (2011) [arXiv:1006.2359 [hep-ph]].
[25] S. Galais and C. Volpe, Phys. Rev. D **84**, 085005 (2011) [arXiv:1103.5302 [astro-ph.SR]].
[26] H. Duan, G. M. Fuller, J. Carlson and Y. -Z. Qian, Phys. Rev. Lett. **100**, 021101 (2008) [arXiv:0710.1271 [astro-ph]].
[27] G. L. Fogli, E. Lisi, A. Marrone and A. Mirizzi, JCAP **0712**, 010 (2007) [arXiv:0707.1998 [hep-ph]].
[28] S. Choubey, B. Dasgupta, A. Dighe and A. Mirizzi, arXiv:1008.0308 [hep-ph].
[29] H. Duan, G. M. Fuller, J. Carlson and Y. -Z. Qian, Phys. Rev. Lett. **97**, 241101 (2006) [astro-ph/0608050].
[30] G. Raffelt, S. Sarikas and D. d. S. Seixas, Phys. Rev. Lett. **111**, 091101 (2013) [arXiv:1305.7140 [hep-ph]].
[31] A. Mirizzi, Phys. Rev. D **88**, 073004 (2013) [arXiv:1308.1402 [hep-ph]].
[32] H. Duan, G. M. Fuller, J. Carlson and Y. -Z. Qian, Phys. Rev. D **74**, 105014 (2006) [astro-ph/0606616].
[33] S. Pastor, G. G. Raffelt and D. V. Semikoz, Phys. Rev. D **65**, 053011 (2002) [hep-ph/0109035].
[34] H. Duan, G. M. Fuller, J. Carlson and Y. -Z. Qian, Phys. Rev. D **75**, 125005 (2007) [astro-ph/0703776].
[35] B. Dasgupta, A. Dighe, A. Mirizzi and G. G. Raffelt, Phys. Rev. D **77**, 113007 (2008) [arXiv:0801.1660 [hep-ph]].
[36] S. Hannestad, G. G. Raffelt, G. Sigl and Y. Y. Y. Wong, Phys. Rev. D **74**, 105010 (2006) [Erratum-ibid. D **76**, 029901 (2007)] [astro-ph/0608695].
[37] M. B. Deaton, M. D. Duez, F. Foucart, E. O'Connor, C. D. Ott, L. E. Kidder, C. D. Muhlberger and M. A. Scheel *et al.*, Astrophys. J. **776**, 47 (2013) [arXiv:1304.3384 [astro-ph.HE]].
[38] K. Kiuchi, Y. Sekiguchi, K. Kyutoku and M. Shibata, Class. Quant. Grav. **29**, 124003 (2012) [arXiv:1206.0509 [astro-ph.HE]].
[39] A. Malkus, J. P. Kneller, G. C. McLaughlin and R. Surman, Phys. Rev. D **86**, 085015 (2012) [arXiv:1207.6648 [hep-ph]].
[40] H. Duan, G. M. Fuller and Y. -Z. Qian, Phys. Rev. D **74**, 123004 (2006) [astro-ph/0511275].
[41] F. P. An *et al.* [Daya Bay Collaboration], Phys. Rev. Lett. **112**, 061801 (2014) [arXiv:1310.6732 [hep-ex]].
[42] C. Lunardini and A. Y. Smirnov, JCAP **0306**, 009 (2003) [hep-ph/0302033].
[43] A. S. Dighe and A. Y. Smirnov, Phys. Rev. D **62**, 033007 (2000) [hep-ph/9907423].

[44] O. L. Caballero, G. C. McLaughlin, and R. Surman Phys. Rev. D **80**, 123004 (2009) [arXiv:0910.1385 [astro-ph.HE]].
[45] S. Galais, J. Kneller and C. Volpe, J. Phys. G **39**, 035201 (2012) [arXiv:1102.1471 [astro-ph.SR]].
[46] J. P. Kneller and G. C. McLaughlin, Phys. Rev. D **80**, 053002 (2009) [arXiv:0904.3823 [hep-ph]].
[47] B. Dasgupta, A. Dighe, A. Mirizzi and G. G. Raffelt, Phys. Rev. D **78**, 033014 (2008) [arXiv:0805.3300 [hep-ph]].
[48] J. Beringer *et al.* [Particle Data Group Collaboration], Phys. Rev. D **86**, 010001 (2012).
[49] B. D. Metzger and E. Berger, Astrophys. J. **746**, 48 (2012) [arXiv:1108.6056 [astro-ph.HE]].
[50] J. F. Cherry, J. Carlson, A. Friedland, G. M. Fuller and A. Vlasenko, Phys. Rev. D **87** (2013) 085037 [arXiv:1302.1159 [astro-ph.HE]].